

ORIGINAL ARTICLE

Chemokine C-C motif ligand 21 synergized with programmed death-ligand 1 blockade restrains tumor growth

Qiangda Chen^{1,2}  | Hanlin Yin^{1,2} | Ning Pu^{1,2}  | Jicheng Zhang^{1,2} | Guochao Zhao^{1,2} | Wenhui Lou^{1,2} | Wenchuan Wu^{1,2} 

¹Department of General Surgery, Zhongshan Hospital, Fudan University, Shanghai, China

²Cancer Center, Zhongshan Hospital, Fudan University, Shanghai, China

Correspondence

Wenchuan Wu and Wenhui Lou, Department of General Surgery, Zhongshan Hospital, Fudan University, 180 Fenglin Road, Shanghai 200032, China.
Email: wu.wenchuan@zs-hospital.sh.cn (WW); lou.wenhui@zs-hospital.sh.cn (WL)

Funding information

China Postdoctoral Science Foundation, Grant/Award Number: 2021M690037; Shanghai Sailing Program, Grant/Award Number: 21YF1407100; National Key R&D Program, Grant/Award Number: 2019YFC1315902; Shanghai ShenKang Hospital Development Centre, Grant/Award Number: SHDC2020CR2017B.

Abstract

Programmed death-ligand 1 (PD-L1) blockade has revolutionized the prognosis of several cancers, but shows a weak effect on pancreatic cancer (PC) due to poor effective immune infiltration. Chemokine C-C motif ligand 21 (CCL21), a chemokine promoting T cell immunity by recruiting and colocalizing dendritic cells (DCs) and T cells, serves as a potential antitumor agent in many cancers. However, its antitumor response and mechanism combined with PD-L1 blockade in PC remain unclear. In our study, we found CCL21 played an important role in leukocyte chemotaxis, inflammatory response, and positive regulation of PI3K-AKT signaling in PC using Metascape and gene set enrichment analysis. The CCL21 level was verified to be positively correlated with infiltration of CD8⁺ T cells by the CIBERSORT algorithm, but no significant difference in survival was observed in either The Cancer Genome Atlas or the International Cancer Genome Consortium cohort when stratified by CCL21 expression. Additionally, we found the growth rate of allograft tumors was reduced and T cell infiltration was increased, but tumor PD-L1 abundance elevated simultaneously in the CCL21-overexpressed tumors. Then, CCL21 was further verified to increase tumor PD-L1 level through the AKT-glycogen synthase kinase-3 β axis in human PC cells, which partly impaired the antitumor T cell immunity. Finally, the combination of CCL21 and PD-L1 blockade showed superior synergistic tumor suppression in vitro and in vivo. Together, our findings suggested that CCL21 in combination with PD-L1 blockade might be an efficient and promising option for the treatment of PC.

KEYWORDS

CCL21, combination therapy, pancreatic cancer, PD-L1, T cell infiltration

Abbreviations: CCL21, chemokine C-C motif ligand 21; CCR7, CC-chemokine receptor 7; GSEA, Gene Set Enrichment Analysis; GSK-3 β , glycogen synthase kinase-3 β ; ICB, immune checkpoint blockade; ICGC, International Cancer Genome Consortium; IL, interleukin; NK, natural killer; OS, overall survival; PC, pancreatic cancer; PD-1, programmed death-1; PD-L1, programmed death-ligand 1; qRT-PCR, quantitative real-time PCR; TCGA, The Cancer Genome Atlas; TIIC, tumor-infiltrating immune cell.

Qiangda Chen, Hanlin Yin, and Ning Pu contributed equally to this work.

This is an open access article under the terms of the Creative Commons Attribution-NonCommercial-NoDerivs License, which permits use and distribution in any medium, provided the original work is properly cited, the use is non-commercial and no modifications or adaptations are made.

© 2021 The Authors. *Cancer Science* published by John Wiley & Sons Australia, Ltd on behalf of Japanese Cancer Association.

1 | INTRODUCTION

Pancreatic cancer is one of the most aggressive and refractory malignant tumors with a 5-year survival of approximately 10%.¹ Traditional treatments for PC, including surgical resection, chemotherapy, and radiotherapy, show limited efficacy, and there are no new effective treatments available. In the past 20 years, the treatment in various cancers has been revolutionized by the development of immunotherapies.^{2,3} Immunotherapies for PC have shown glimmers of promise, but their efficacy remains limited.⁴ Developing rational combination therapies could be crucial to maximizing the therapeutic effect of immunotherapy.

Immune checkpoint blockade therapy, as one of the immunotherapies, has been proved to improve survival in several cancers, including melanoma and lung cancer.⁵⁻⁷ Among all immune checkpoints, the PD-1/PD-L1 axis has emerged as the best candidate target because of its efficacy proven in a large number of cancers.⁸ However, a majority of patients with PC were unresponsive to monotherapy due to the inhibitory immune microenvironment, poor T cell infiltration, and low mutational burden.⁹ Therefore, the current studies attempted to combine ICB with surgery, chemotherapy, radiotherapy, target therapy, or other immunotherapies to overcome the resistance to ICB.

In the past few decades, a huge number of studies found that chemokines could mediate different immune cell subsets trafficking into the tumor environment through binding the corresponding chemokine receptors, affecting tumor progression and therapeutic responses.¹⁰ Therefore, therapies that target specific chemokines or chemokine receptors could achieve clinical benefits in patients with cancer. Among them, CCL21 is the only chemokine listed by the NCI as one of the top 20 agents with high potential for use in cancer therapy. It is predominantly expressed by high endothelial venules in lymph nodes, secondary lymph organs, and spleen,¹¹ and recruits immune cells, such as mature DCs and naive and memory T cells by binding to its chemokine receptor CCR7. In preclinical mouse models, CCL21 was shown to mediate potent antitumor activity through recruiting and colocalizing NK cells, DCs, and T cells in cancers.¹²⁻¹⁴ Effective immunotherapeutic strategies and improvements based on CCL21 emerged to enhance antitumor effects.¹⁵ Recently, a phase I study was undertaken using CCL21 gene-modified DC (CCL21-DC) therapy in lung cancer and the results showed that intratumoral vaccination with CCL21-DCs could significantly enhance the CD8⁺ T cell infiltration, antitumor immune response, and PD-L1 expression.¹⁶ Kadam et al reported that PD-1 immune checkpoint blockade promoted CCL21-DC tumor lysate vaccine to reduce tumor burden in a lung cancer preclinical model.¹⁷ Nevertheless, the roles of CCL21 and its antitumor response combined with ICB therapy in PC remain unclear.

In this study, we found that CCL21 was positively correlated with CD8⁺ T cell infiltration in PC by bioinformatics analysis. However, no significant difference in survival was found between patients with high and low CCL21 expression in both publicly available cohorts. We verified the overexpression of CCL21 in cancer cells with

enhanced T cell infiltration, antitumor immune effects, and PD-L1 expression with the subcutaneous PC model in immune-competent mice. Considering the previous study,^{16,17} we speculated that the antitumoral immune response of CCL21 might be partially blocked by the upregulation of PD-L1 on PC cells. The mechanism of CCL21 upregulating PD-L1 expression through the AKT-GSK-3 β signaling cascade was then verified. Because both high PD-L1 abundance and T cell infiltration in cancers were potential predictive indicators for the response to PD-1/PD-L1 blockade therapy,⁹ the combination of CCL21 with PD-L1 blockade was carried out and showed superior synergistic tumor suppression *in vitro* and *in vivo*. This study provided a rationale for combined CCL21 and PD-L1 blockade as an efficient and promising therapeutic strategy for PC.

2 | MATERIALS AND METHODS

2.1 | Data collection and preprocessing

The transcriptome expression profiles and relevant clinical information of PC were obtained from TCGA (<https://cancergenome.nih.gov/>) and ICGC (<https://dcc.icgc.org/>). The expression data in the TCGA were HTseq-FPKM type, including 178 PC samples and four normal samples. Cases with insufficient TNM stage or follow-up period less than 30 days were excluded. Finally, 168 cases with detailed clinical information from the TCGA database were included as previously described.¹⁸ The gene expression microarray dataset PACA-AU, including 269 PC samples with survival information, was enrolled as the validation cohort.

2.2 | Functional enrichment analysis by GeneMANIA and GSEA

GeneMANIA (<http://www.genemania.org>), a useful online platform,¹⁹ was applied to construct and visualize a gene-gene interaction network and functional analysis for CCL21 by the bioinformatics methods, including physical interactions, coexpression, website prediction, colocalization, pathways, genetic interactions, and shared protein domains.

Gene Set Enrichment Analysis²⁰ was further used to investigate whether an a priori defined set of genes were significantly differentially expressed between high and low CCL21 expression groups in the TCGA cohort according to the median of gene expression. The selected gene set was c5.go.bp.v7.2.symbols. The gene set was significantly enriched, with a normal *P* value less than .05 and a false discovery rate less than 0.05.

2.3 | Analysis of tumor immune microenvironment

CIBERSORT, an analytical tool developed by Newman et al,²¹ was used to assess the immune cell infiltrations of the tumoral samples

from the TCGA and ICGC cohort based on normalized gene expression profiles. The standardized processed dataset of gene expression was uploaded to the CIBERSORT website (<https://cibersort.stanford.edu/index.php>) to analyze using 100 aligned default signature matrices. To improve the accuracy of the algorithm, Monte Carlo sampling was used for the deconvolution of each sample to get a CIBERSORT *P* value, and only samples with a CIBERSORT *P* value less than .05 were considered eligible for analysis, as previously described.¹⁸

2.4 | Cell lines and culture

The human pancreatic cancer cell lines MIA-PaCa-2 and SW1990 were obtained from the Chinese Academy of Science. Murine pancreatic cancer cells Panc02 were a kind gift from Johns Hopkins Hospital. MIA-PaCa-2 cells were maintained in high-glucose DMEM (Gibco) with 10% FBS (Gibco) and 2.5% horse serum (Solarbio Life Sciences). SW1990 cells were incubated in Leibovitz's L-15 Medium (Gibco) with 10% FBS, and Panc02 cells were cultured in RPMI-1640 medium (Gibco) supplemented with 10% FBS. All cells were kept in an incubator at 37°C with 5% CO₂.

2.5 | Cell transfection

The Ubi-MCS-3FLAG-CBh-gcGFP-IRES-puromycin lentiviral vector was obtained and used as a control from GeneChem. The lentiviral vector was constructed containing Ubi-Ccl21-3FLAG-CBh-gcGFP-IRES-puromycin. The primer sequences for the mouse CCL21 gene fragment were 5'-AGGTCGACTCTAGAGGATCCGCCACCATGGCTCAGATGATGACTCTGAG-3' (forward) and 5'-TCCTTGAGTCCATCCTCTCTGAGGGCTGTGTCTG-3' (reverse). The CCL21 expression after transfection was confirmed by qRT-PCR, western immunoblot analysis, and ELISA.

2.6 | RNA isolation, reverse transcription, and qRT-PCR

The total RNAs of pancreatic cancer cells were extracted by TRIzol Reagent (Invitrogen). cDNA was prepared with PrimeScript reverse transcriptase Master Mix (Takara Bio). SYBR Premix Ex Taq and gene-specific primers were used for PCR amplification and detection on ABI QuantStudio5. The sequences of primers were as follows: human PD-L1, 5'-CCAGGATGGTTCTTAGACTCCC-3' (forward) and 5'-TTTAGCACGAAGCTCTCCGAT-3' (reverse); human GAPDH, 5'-CAACAGCTCAAGATCATCAGC-3' (forward) and 5'-ATGAGTCC TTCCACGATACCAA-3' (reverse); mouse Ccl21, 5'-ATCCCGCAAT CCTGTTCT-3' (forward) and 5'-AGTTCTTGCAGCCCTTGG-3' (reverse); and mouse Gapdh, 5'-GCCGAGAATGGGAAGCTTGTC-3' (forward) and 5'-TCCACGACATACTCAGCACCG-3' (reverse). The qPCR data were normalized to GAPDH or Gapdh using the 2^{-ΔΔCt} method.

2.7 | Immunoassays

Supernatants were collected from the cultured Panc02 cells after transfection and stored at -80°C for further studies. The CCL21 concentration was measured by the Mouse CCL21 ELISA Kit (Boster Biological Technology). The procedures were carried out according to the product instruction.

2.8 | Western blot analysis and coimmunoprecipitation assays

Cells were lysed in the RIPA buffer (Beyotime) containing 1% Protease/Phosphatase Inhibitor Cocktail (MCE) and PMSF. The BCA Protein Assay Kit (Epizyme) was applied to measure protein concentrations. Western blot analysis was carried out as previously described.²² For coimmunoprecipitation assays, MIA-PaCa-2 and SW1990 cells were transfected with the indicated plasmids according to manual of Lipofectamine 3000's manufacturer (Sigma-Aldrich). Immunoprecipitation was undertaken as described previously.^{22,23} In this study, anti-PD-L1 (ab228415) was purchased from Abcam. Anti-phospho-AKT (Ser473)(9271), anti-AKT (9272), anti-phospho-GSK-3β (ser9)(9323), anti-GSK-3β (12456), anti-GAPDH (5174), and anti-β-actin (4970) were purchased from Cell Signaling Technology. Anti-Ccl21 (AF457-SP) and anti-CCR7 (150503) were purchased from R&D Systems.

2.9 | In vivo mouse studies

Six-week-old female C57BL/6 mice were purchased from Shanghai Jie Si Jie Laboratory Animal Co., Ltd. The mice were maintained under pathogen-free conditions. All procedures were approved by the institutional review board of Zhongshan Hospital, Fudan University. Mice were subcutaneously injected in the back with 2 × 10⁶ stable CCL21-OE or vector control Panc02 cells. Seven days later, mice were pooled and randomly divided into different groups with comparable average tumor size. Immunoglobulin G isotype control Ab or PD-L1 Ab (Bio X cell) was intraperitoneally injected with 100 μg/mouse every 72 hours. Tumors were measured every 3 days. Tumor volume was calculated by 1/2ab², where a represented the long tumor diameter and b represented the short tumor diameter.

2.10 | Immunohistochemistry and immunofluorescence

Hematoxylin-eosin staining was carried out in formalin-fixed, paraffin-embedded mouse tumor specimens. Anti-PD-L1 (14-5982-82; Invitrogen), anti-CD4 (ab183685; Abcam), anti-CD8 (ab217344; Abcam), anti-Ccl21 (AF457-SP; R&D Systems), and anti-Granzyme B (ab4059; Abcam) Abs were applied for IHC staining as previously described.²² Immunofluorescence was carried out according to the TUNEL Apoptosis Detection Kit (Beyotime) product instruction.

2.11 | Flow cytometry analysis

The PD-L1-APC Ab (BD Biosciences) was used to examine the PD-L1 expression on the surface of untreated and treated pancreatic cancer cell lines after incubating for 30 minutes in PBS plus 2% FBS. The target populations were identified by FACS Aria II flow cytometer (BD Biosciences). The data were processed using FlowJo software.

2.12 | T cell-mediated tumor cell killing assay

Ficoll reagent (Stemcell) was applied to separate PBMCs from healthy donors using density-gradient centrifugation. The PBMCs were cultured in RPMI-1640 medium for 2 hours. The adherent cells (immature DCs) were cultured in RPMI-1640 medium with granulocyte macrophage colony-stimulating factor (100 ng/mL; PeproTech) and IL-4 (100 ng/mL; PeproTech) for 5 days, and tumor necrosis factor- α (50 ng/mL; PeproTech) was then added to induce DC maturation for 2 days. Tumor cell lysates were obtained by rapid freezing in liquid nitrogen and thawing in a 37°C water bath repeatedly as previously described.²⁴ The mature DCs were cocultured with the relevant tumor cell lysates for 3 days to generate the DCs loaded with tumor antigen.

The Pan T Cell Isolation Kit (Miltenyi Biotec) was further used to separate T cells from nonadherent cells. T cells were cultured and preactivated with RPMI-1640 medium containing recombinant human IL-2 (10 ng/mL), anti-CD3 Ab (10 μ g/mL; BioLegend), and anti-CD28 Ab (10 μ g/mL; BioLegend). The T cells were then mixed with the DCs loaded with tumor antigen at a ratio of 10:1 in the RPMI-1640 medium with IL-12 (100 ng/mL; PeproTech) for 3 days to generate tumor cell line-specific T cells.²⁴ For the T cell-mediated tumor cell killing assay, MIA-PaCa-2 and SW1990 cells were seeded in 12-well plates and prestimulated with 100 ng/mL CCL21 (PeproTech) or PBS for 48 hours. T cells were then directly added into the wells at a ratio of 6:1. Anti-human PD-L1 or IgG isotype (20 μ g/mL; Bio X cell) as control were used to block cancer cell endogenous PD-L1. After 4 days of T cell and tumor cell coculturing, the wells were washed with PBS three times to remove dead tumor cells and T cells. The surviving tumor cells were fixed and stained with a crystal violet solution. To further mimic the chemotactic effect of CCL21 in vitro, we modified the T cell-mediated tumor cell killing assay using the Transwell system (5 μ m pore size; Labselect). Pancreatic cancer cells were seeded in the lower chamber prior to the addition of the relevant tumor cell line-specific T cells in the upper chamber at a ratio of 1:10. The remaining procedures were carried out as described above.

2.13 | Statistical analysis

SPSS 22.0 software (IBM Corporation), R 3.6.3 (R Foundation for Statistical Computing), and GraphPad Prism 6.0 (GraphPad Software)

were used for statistical analysis and diagram construction. The correlations between CCL21 expression and clinicopathologic characteristics were analyzed by Person's χ^2 test or Fisher's exact test. The OS was depicted by Kaplan-Meier survival curves and compared by log-rank tests. The quantitative data of two groups were compared by two-tailed Student's *t* test and multiple comparisons were made by one-way ANOVA. ImageJ software (NIH) was used to analyze the western blot bands. All the experimental results are presented as means \pm SD from three or six independent experiments. *P* < .05 was considered as statistically significant.

3 | RESULTS

3.1 | Interacted genes and enrichment analysis of CCL21

To obtain mechanistic insights into the function of CCL21, the protein-protein interaction network of CCL21 and its functionally related genes was analyzed using GeneMANIA. The gene sets enriched for CCL21 were responsible for G-protein coupled chemoattractant receptor activity, cellular calcium ion homeostasis, leukocyte chemotaxis and apoptotic process, inflammatory response, and positive regulation of protein kinase B signaling (Figure S1A).

To further understand and validate the biological functions of CCL21 in PC, GSEA was applied to identify the gene signatures that were positively correlated with high CCL21 expression in the TCGA cohort. Gene sets associated with regulation of PI3K signaling, epithelial cell apoptotic process, inflammatory response, calcium mediated signaling, leukocyte migration and chemotaxis, phospholipase activity, and immune effector process were significantly enriched in the CCL21 highly-expressed phenotype (Figure S1B). These findings indicated that CCL21 could play a vital role in leukocyte chemotaxis and activation of PI-3K-AKT signaling.

3.2 | Chemokine CCL21 positively associated with CD8⁺ T cell infiltration, but not survival

We then explored whether CCL21 expression was correlated to the infiltration of immune cells in PC using the CIBERSORT algorithm. One hundred and twenty-eight tumor samples with CIBERSORT *P* < .05 were eligible in this study. The landscape of immune infiltration in PC arranged by CCL21 expression from low to high is shown in Figure 1A. To investigate the effect of CCL21 on tumor-infiltrating immune cells, the samples were equally divided into two groups according to the median of CCL21 expression in the TCGA cohort. Compared with the low expression group, the proportions of naive B cells, CD8⁺ T cells, and activated CD4⁺ memory T cells were significantly higher in the CCL21-high expression group, whereas the proportions of activated NK cells and M0 macrophages were relatively lower (all *P* < .05; Figure 1B).

TCGA cohort

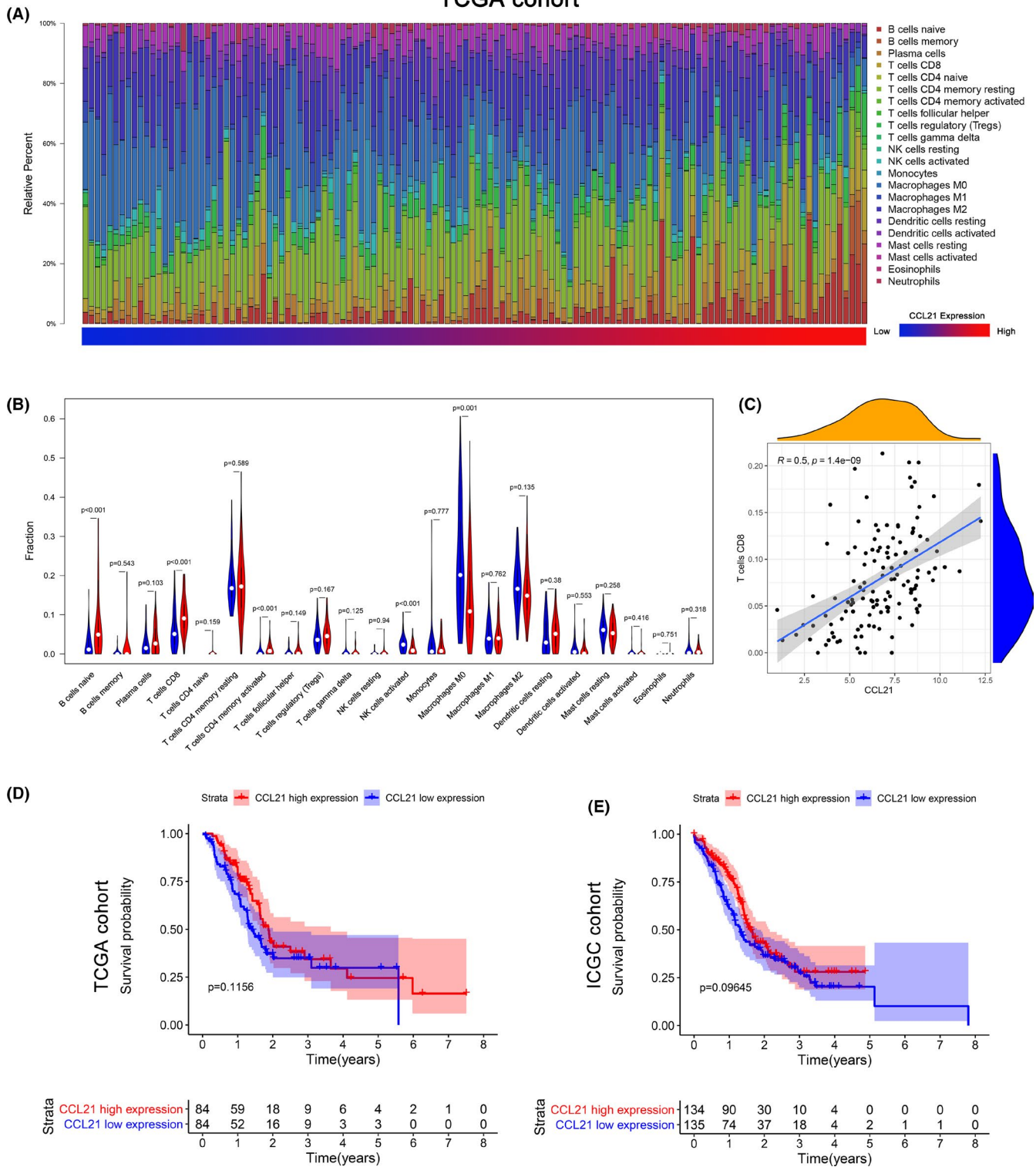


FIGURE 1 Chemokine C-C motif ligand 21 (CCL21) was positively associated with CD8+ T cell infiltration, but not survival. A, The landscape of immune infiltration in 128 tumor tissues arranged by CCL21 expression from low to high in The Cancer Genome Atlas (TCGA) cohort. B, Analysis of differential immune cells between the low and high CCL21 expression group in TCGA cohort. C, Correlation analysis of CCL21 and CD8 T cells based on TCGA data. Kaplan-Meier survival curves of CCL21 in (D) TCGA and (E) International Cancer Genome Consortium (ICGC) cohorts

To avoid bias from one single cohort, PACA-AU was used as a validation cohort. One hundred and seventy-eight tumor samples qualified after they were filtered with CIBERSORT $P < .05$. Likewise, the landscape of immune cells is summarized in Figure S2A. Using the same grouping as the TCGA cohort, the high CCL21 expression group contained more naive B cells, CD8⁺ T cells, resting CD4⁺ T cells, and M1 macrophages compared with the low expression group, while the infiltration of activated CD4⁺ T cells and M0 macrophages was significantly lower (all $P < .05$; Figure S2B). We then investigated the correlation of CCL21 expression and differential infiltration of immune cells in both TCGA and ICGC cohorts, and only CD8⁺ T cells were found to be moderately correlated with CCL21 expression ($R = .5$, $P = 1.4e-09$ and $R = .33$, $P = 6.4e-06$, Figure 1C and Figure S2C). These results strongly confirmed that CCL21 expression was positively associated with T cell infiltration.

In addition, the median OS for the CCL21 high-expression group was 22.5 months, higher than that for the CCL21 low-expression group (16.8 months) in the TCGA cohort ($P = .12$; Figure 1D). Similarly, the median OS stratified by the CCL21 level in the ICGC cohort was 19.3 and 15.7 months, respectively ($P = .10$; Figure 1E). Although the patients with higher expression of CCL21 tended to have higher survival rates in both TCGA and ICGC cohorts, no significant difference was observed. The correlations between CCL21 expression and other clinicopathologic characteristics are summarized in Table S1, and the results showed that only tumor site was significantly correlated with CCL21 ($P = .021$). Collectively, our findings suggested that CCL21 could potentially enhance local tumor immune response, but no obvious survival benefit was observed.

3.3 | Chemokine CCL21 promoted T cell infiltration and increased PD-L1 expression in vivo

According to the above results, T cell infiltration induced by CCL21 was further validated in a murine model of PC. The CCL21-overexpressed Panc02 cells by the lentiviral vector were constructed and validated by the upregulation of CCL21 mRNA and protein expression (Figure 2A-C). The CCL21-overexpressed Panc02 cells and control Panc02 cells were incubated into C57BL/6 mice. Overexpression of CCL21 significantly reduced tumor volume and weight compared with the control group ($P < .05$; Figure 2D). The numbers of tumor-infiltrating CD4⁺ and CD8⁺ T cells and apoptotic cells were increased in the CCL21-overexpressed tumors compared with control tumors (Figure 2E,F). Moreover, tumors that developed from transplanted CCL21-overexpressed Panc02 cells remained CCL21-positive, with concomitant PD-L1 upregulation (Figure 2E), which implied that PD-L1 upregulation might partly impair the antitumor immunity mediated by CCL21 chemotactic T cells.

3.4 | Chemokine CCL21 upregulated PD-L1 expression to promote immune escape in vitro

To further investigate whether CCL21 could induce PD-L1 expression in human PC, MIA-PaCa-2 and SW1990 cell lines were treated with CCL21. The protein levels of PD-L1 were increased in both time- and dose-dependent manners by CCL21 stimulation (Figure 3A,B). The upregulation of cell-surface PD-L1 expression induced by CCL21 was further validated using flow cytometric analysis (Figure 3C). However, CCL21 had no effects on PD-L1 mRNA expression compared with the untreated cells (Figure 3D), which implied that CCL21-induced PD-L1 might be primarily at the post-translational level, not at transcription activation. Given that binding of PD-L1 to PD-1 inhibited the activation of T cells,²⁵ it was further investigated whether CCL21-enhanced PD-L1 levels in PC could inhibit T cell cytotoxicity. T cell cytotoxicity assay was carried out and results showed that CCL21-stimulated tumor cells could prevent themselves from T-cell killing to some degree, while PD-L1 blockade could mostly rescue this effect (Figure 3E), suggesting that PD-L1 expression enhanced by CCL21 could induce immune escape from T-cell killing. To mimic the chemotactic role of CCL21 in vitro, a modified T cell-mediated tumor cell killing assay using the Transwell system was further applied. The combination of CCL21 and anti-PD-L1 Ab increased the cytotoxic activity for pancreatic cancer cells in vitro (Figure 3F).

3.5 | Chemokine CCL21 stabilized PD-L1 through AKT-GSK-3 β signaling pathway

Next, the specific mechanism of CCL21 enhancing PD-L1 expression was further investigated. In the presence of protein synthesis inhibitor cycloheximide, CCL21 increased the PD-L1 protein half-life in both cell lines, which also implied that CCL21 could stabilize PD-L1 protein at the posttranslational level (Figure 4A). Previously, a study had reported that GSK-3 β could phosphorylate and downregulate PD-L1 protein stability, and phosphorylation and inactivation of GSK-3 β at Ser9 could stabilize PD-L1 expression in breast cancer cells.²³ Through the functional enrichment analysis of CCL21, we observed that positive regulation of PI3K-AKT signaling was significantly enriched in high CCL21 groups, while GSK-3 β was thought to be a downstream protein in AKT signaling pathway.^{26,27} For these reasons, we speculated that CCL21 might stabilize PD-L1 expression by activating the AKT signaling pathway and then suppressing GSK-3 β activity through Ser9 phosphorylation.

To test our hypothesis, the effect of CCL21 on the AKT-GSK-3 β signaling pathway was assessed by measuring these substrates and their phosphorylation. The results showed that CCL21 significantly phosphorylated AKT and GSK-3 β (Ser9) in both PC cell lines (Figure 4B). To identify whether the AKT-GSK-3 β signaling pathway was responsible

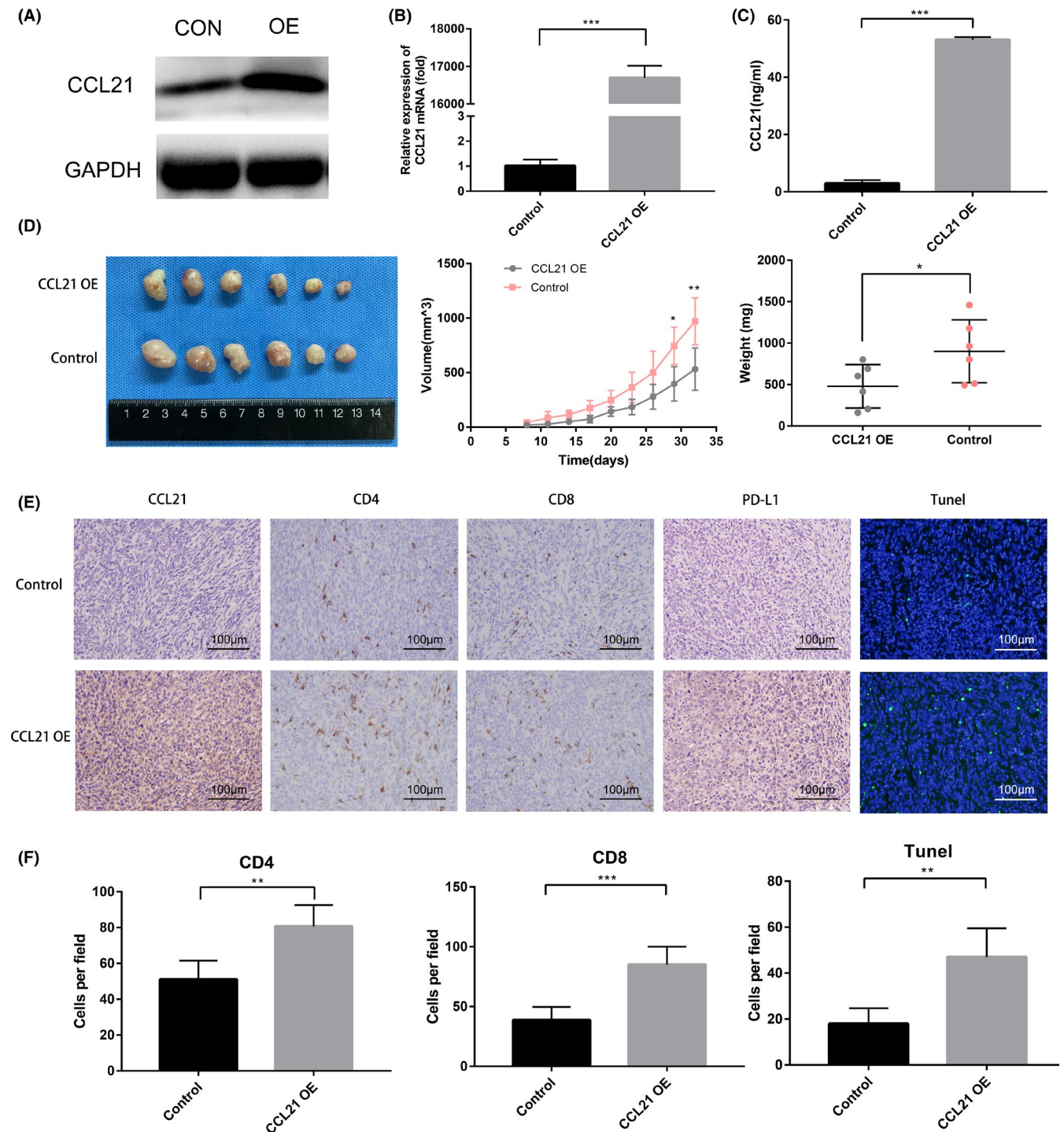


FIGURE 2 Chemokine C-C motif ligand 21 (CCL21) promoted T cell infiltration as well as increased programmed death-ligand 1 (PD-L1) expression in vivo. A-C, (A) Western blot analysis, (B) quantitative real-time PCR analysis, and (C) ELISA analysis for CCL21 in CCL21 overexpressing (OE) and relative control Panc02 (CON) cells. D, Images (left), volumes (middle), and weights (right) of the CCL21 OE vs control Panc02 tumors in C57BL/6 mice. E, Immunohistochemical images of CCL21 and PD-L1 expression levels and tumor-infiltrating lymphocyte densities, and immunofluorescent images of TUNEL staining in CCL21 OE vs control Panc02 tumors in C57BL/6 mice. Representative images are shown. Scale bars, 100 μm. F, Quantification of immunohistochemistry and immunofluorescence results of CD4⁺ T cells, CD8⁺ T cells, and TUNEL⁺ cells in CCL21 OE vs control Panc02 tumors in C57BL/6 mice. Each group contained six mice. Statistical significance was calculated by unpaired two-tailed Student's *t* tests. ***P* < .01, ****P* < .001

for the upregulation of PD-L1, MIA-PaCa-2 and SW1990 cells were pretreated with the specific inhibitor of AKT (LY294002), and results revealed that LY294002 remarkably abolished CCL21-induced

GSK-3β phosphorylation and PD-L1 upregulation (Figure 4C,D). Moreover, the coimmunoprecipitation assay was used to further validate that PD-L1 could interact with GSK-3β endogenously in PC

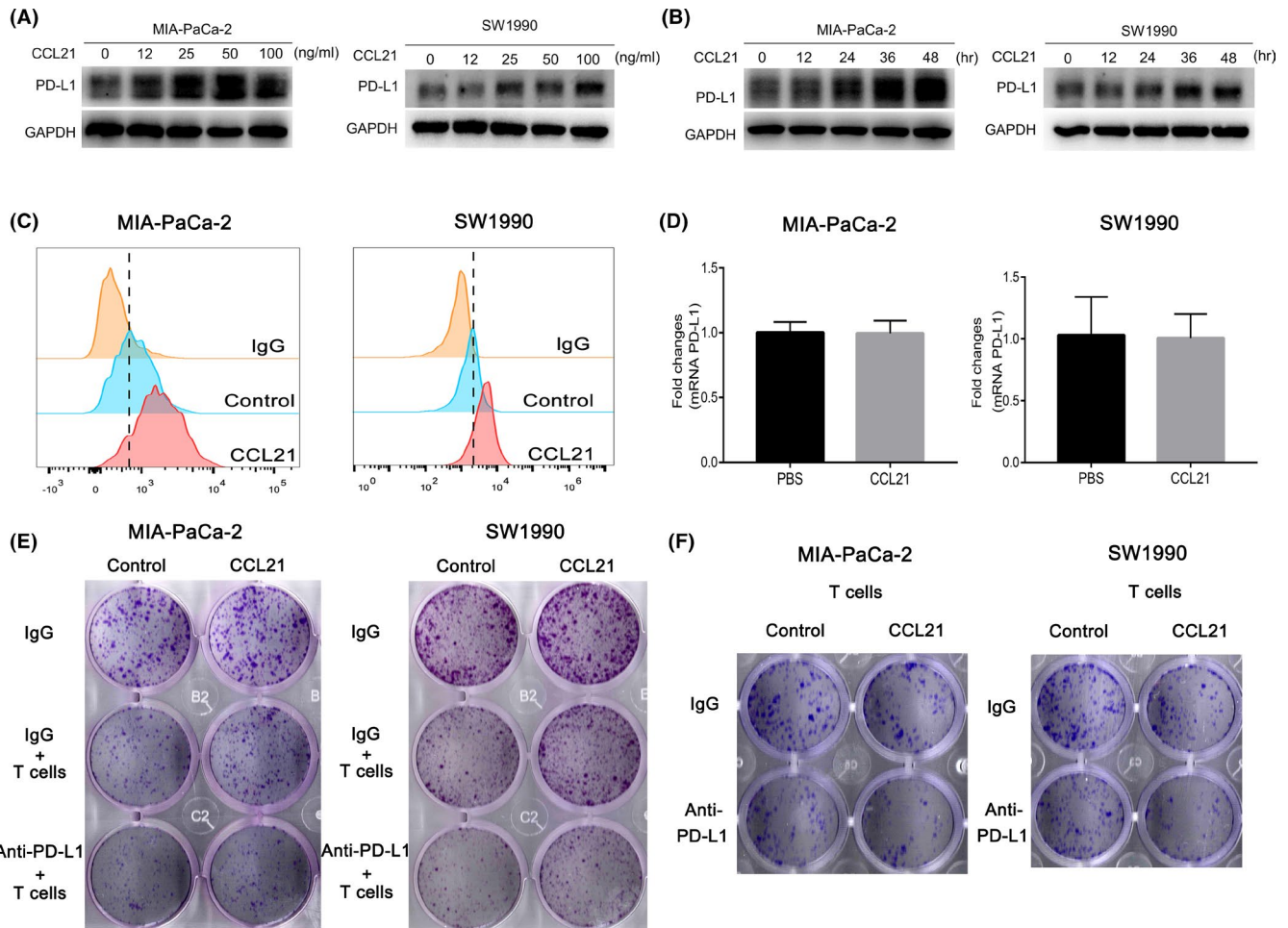


FIGURE 3 Chemokine C-C motif ligand 21 (CCL21) upregulated programmed death-ligand 1 (PD-L1) expression to promote immune escape in vitro. **A**, Western blot analysis of PD-L1 abundance in MIA-PaCa-2 and SW1990 cells treated with CCL21 at the concentration of 0, 12, 25, 50, or 100 ng/mL for 48 h. **B**, Western blot analysis of PD-L1 abundance in MIA-PaCa-2 and SW1990 cells treated with CCL21 at a concentration of 50 ng/mL for 0, 12, 24, 36, and 48 h after 24 h starvation. **C**, Flow cytometry analysis of PD-L1 expression in MIA-PaCa-2 and SW1990 cells treated with 50 ng/mL CCL21 for 48 h. **D**, Quantitative real-time PCR analysis of PD-L1 mRNA level when MIA-PaCa-2 and SW1990 cells were treated with CCL21 (50 ng/mL) or PBS for 12 h. **E**, T cell-mediated tumor cell killing assay analysis of different groups of cancer cell survival after coculture with or without activated T cells or anti-PD-L1 Ab for 4 d. **F**, Modified T cell-mediated tumor cell killing assay using the Transwell system. Pancreatic cancer cells were seeded in the lower chamber prior to addition of the corresponding tumor cell line-specific T cells in the upper chamber. Surviving tumor cells were visualized by crystal violet staining

(Figure 4E). These results suggested that CCL21 could stabilize PD-L1 in PC through the AKT- GSK-3 β signaling pathway.

3.6 | Chemokine CCL21 combined with PD-L1 blockade therapy enhanced therapeutic efficacy for tumor

Recent studies showed that PD-L1 expression was the most widely used and FDA-approved predictive biomarker of anti-PD-1/PD-L1 therapies.²⁸ Patients with PD-L1 positive tumors could have a higher objective response rate and improved OS compared to PD-L1 negative subgroups.^{29,30} According to the above results, we investigated whether CCL21 could synergize with PD-L1 blockade to elicit an enhanced therapeutic efficacy for PC. The lentiviral vector was used to overexpressed CCL21 in tumor cells to mimic its intratumoral

injection. As expected, treatment of immunocompetent mice harboring CCL21-overexpressed tumors with anti-PD-L1 therapy caused a more noticeable suppressive effect on tumor growth compared with either treatment alone (Figure 5A-C). Furthermore, the number of granzyme B⁺ and apoptotic cells were obviously increased after combination therapy, whereas the infiltration of CD4⁺ and CD8⁺ T cells showed no significant difference between combination therapy and CCL21 overexpression (Figure 5D,E). These results showed anti-PD-L1 therapy in combination with CCL21 could improve antitumor activity and significantly suppress tumor growth.

4 | DISCUSSION

In this study, we systematically analyzed the role of CCL21 in PC by bioinformatics. GeneMANIA and GSEA suggested that CCL21 was

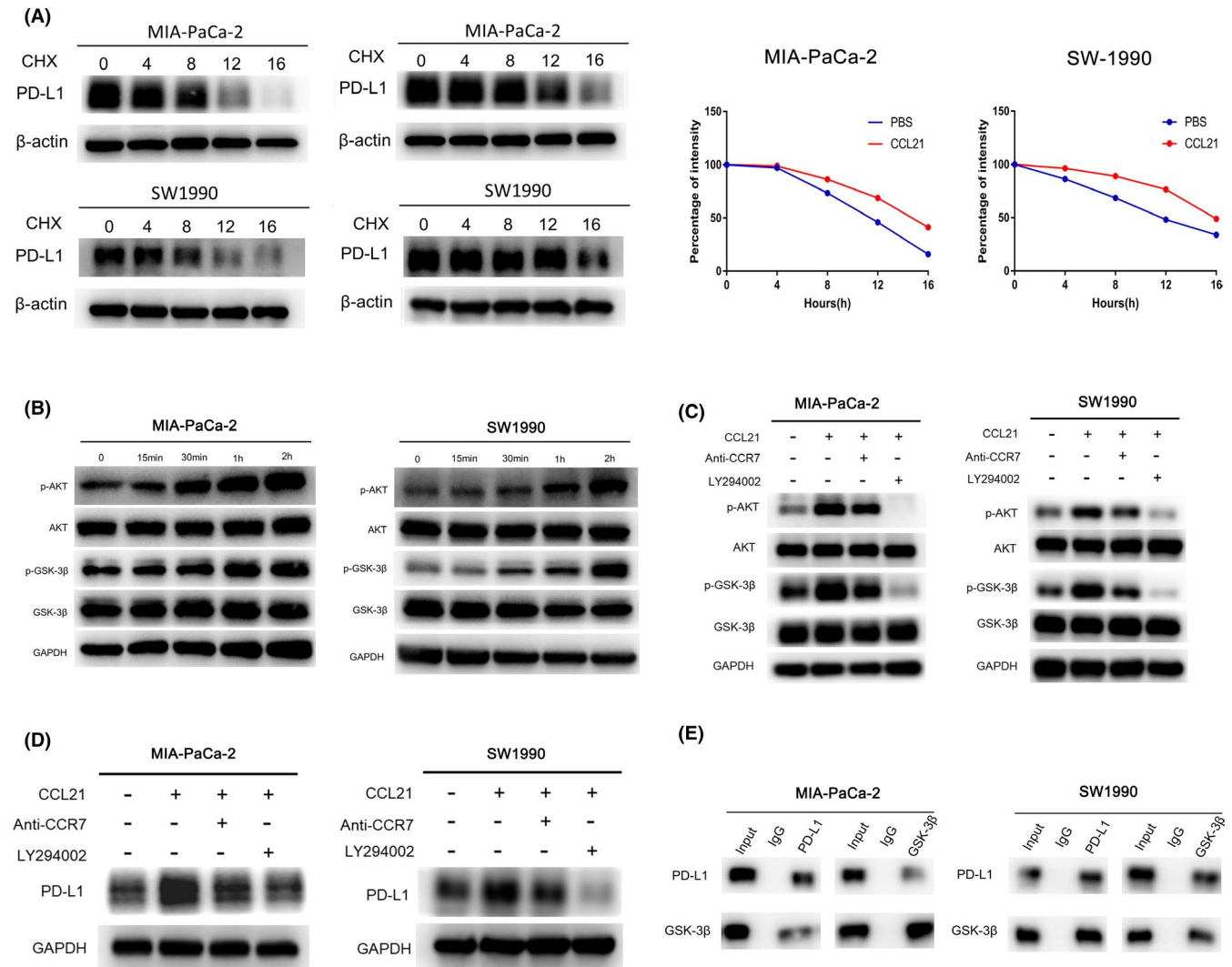


FIGURE 4 Chemokine C-C motif ligand 21 (CCL21) stabilized programmed death-ligand 1 (PD-L1) through the AKT-glycogen synthase kinase-3 β (GSK-3 β) signaling pathway. A, Western blot analysis of PD-L1 abundance in MIA-PaCa-2 and SW1990 cells treated with 80 μ M cycloheximide (CHX) for 0, 4, 8, 12, or 16 h after CCL21 stimulation (right) or not (left). B, Western blot analysis of AKT-GSK-3 β signaling pathway changes of starved cells treated with serum-free medium contained CCL21 (50 ng/mL) for 0, 15, 30, 60, and 120 min. C, Western blot analysis of the AKT-GSK-3 β signaling pathway changes of starved cells pretreated with DMSO, AKT inhibitor (LY294002, 20 μ mol/L) or anti-CCR7 (10 μ g/mL) for 2 h, and then treated with CCL21 (50 ng/mL) or PBS for an additional 2 h. D, Western blot analysis of PD-L1 expression in starved cells pretreated with DMSO, LY294002 or anti-CCR7 for 2 h, and then treated with CCL21 (50 ng/mL) or PBS for an additional 48 h. E, Coimmunoprecipitation assays in MIA-PaCa-2 and SW1990 cells transfected with indicated plasmids

associated with leukocyte chemotaxis and inflammatory response in PC as described in previous studies.^{15,31} Moreover, calcium-mediated signaling and PI3K signaling have also been reported as common signaling pathways of CCR7 elicited by CCL21.³² To investigate the effect of CCL21 on TIICs in PC, CIBERSORT was applied to compare the TIICs between low and high CCL21 expression groups. Only the immune cells significantly altered and correlated with CCL21 expression in both TCGA and ICGC cohorts were selected for further focused research to minimize bias and enhance reliability. As expected, CD8⁺ T cells were significantly changed and related to CCL21 expression. Several studies found that the patients with higher infiltration of CD8⁺ T cells in PC tend to have longer OS.^{33,34} Although the patients

with higher CCL21 seemed to be positively correlated with increased OS, no significant survival differences were found in either publicly available cohort. Therefore, we speculated that there might be a potential immune escape partly impairing the efficacy of CCL21.

Previously, a phase I study reported that tumor PD-L1 level was increased after intratumoral vaccination with CCL21-DCs in lung cancer.¹⁶ The PD-L1 expression in PC cells has been reported and varied widely in previous studies.^{35,36} Binding of PD-L1 to PD-1 on activated T cells impedes antitumor immunity. In addition, the chemokine signaling pathway has been found to be involved in the regulation of PD-L1 through the CXCL9/10/11-CXCR3 axis.³⁷ Thus, we tried to investigate whether CCL21 itself could upregulate PD-L1

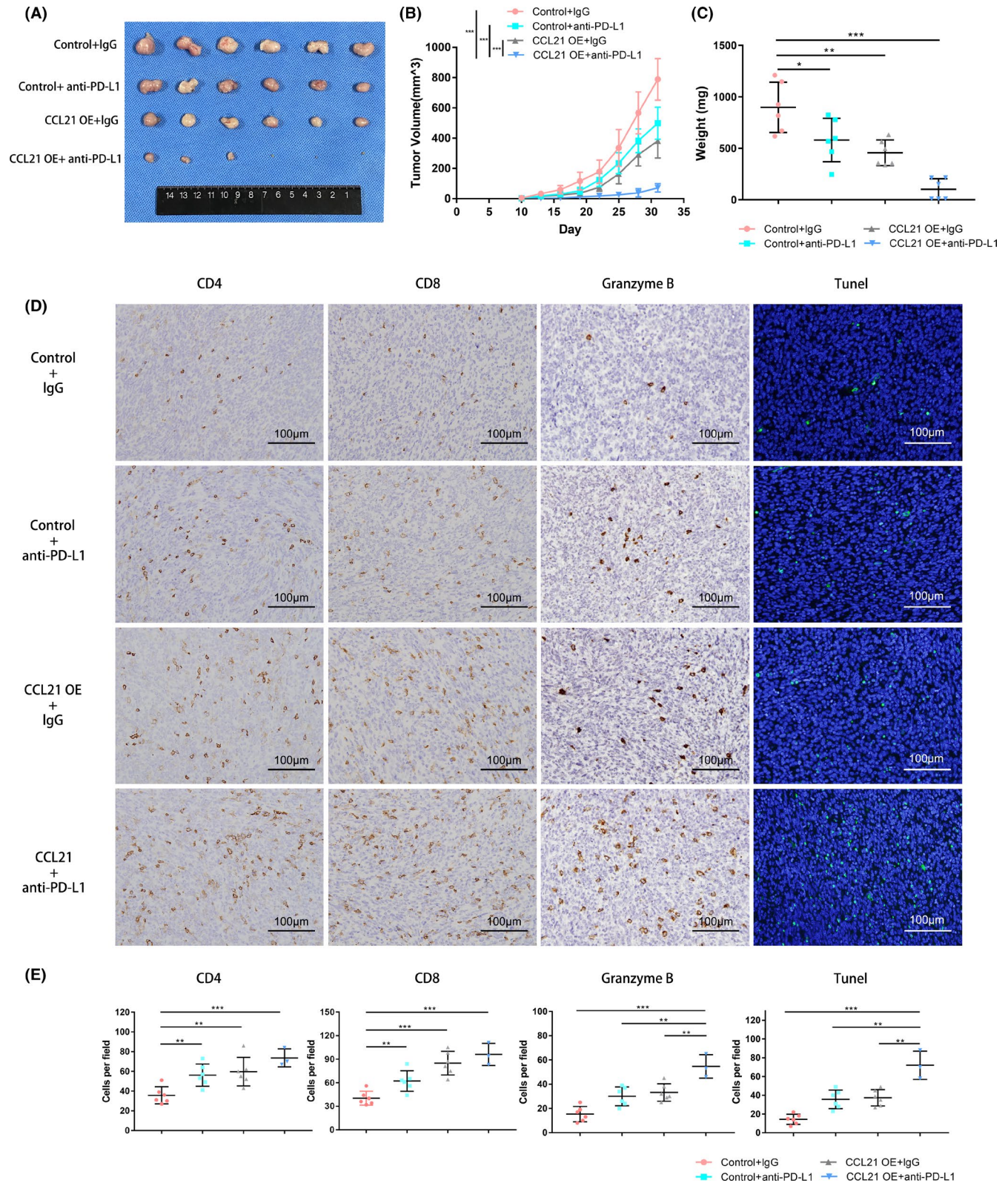
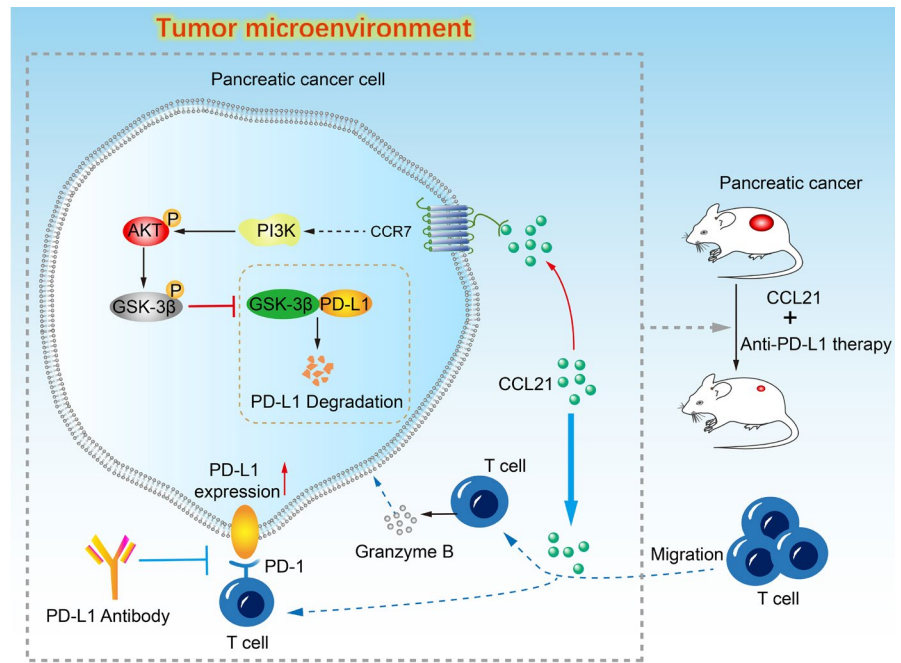


FIGURE 5 Chemokine C-C motif ligand 21 (CCL21) combined with programmed death-ligand 1 (PD-L1) blockade enhanced therapeutic efficacy for pancreatic cancer. A-C, (A) Tumor images, (B) volumes, and (C) weights (means \pm SD) of control Panc02 or CCL21-overexpressing (OE) Panc02 tumor subcutaneously inoculated in C57BL/6 mice treated with IgG control Ab or anti-PD-L1 Ab as indicated. D, Immunohistochemistry analysis of CD4, CD8, and granzyme B, and immunofluorescent image of TUNEL staining in tumors from mice that received the treatments described above. Representative images are shown. Scale bars, 100 μ m. E, Quantification of immunohistochemistry and immunofluorescence results above. Each group contained six mice. Statistical significance was calculated by unpaired two-tailed Student's *t* tests. ***P* < .01, ****P* < .001

FIGURE 6 Schematic drawing for the mechanism of chemokine C-C motif ligand 21 (CCL21) synergistic with programmed death-ligand 1 (PD-L1) blockade. CCL21 in the tumor microenvironment can promote infiltration of T cells and enhance their antitumor immune response. However, CCL21 also stabilizes and upregulates PD-L1 expression on pancreatic cancer cells through the AKT-glycogen synthase kinase-3 β (GSK-3 β) signaling pathway at the same time, which could partly impair the local immune response. Thus, PD-L1 blockade was undertaken in combination with CCL21, which showed a powerful synergism and promising therapeutic efficacy. CCR7, CC-chemokine receptor 7



expression in PC to induce immune evasion. In immune-competent mice, we found that CCL21 overexpression in cancer cells not only enabled the chemotaxis of CD4⁺ and CD8⁺ T cells and the suppression of tumor growth, as previously reported in several cancers,^{12-14,38} but also increased PD-L1 expression. Furthermore, we confirmed that CCL21 could obviously stabilize and upregulate the PD-L1 protein level, but not the mRNA level, in PC cells, which partly hindered the antitumor T immunity. After that, we further investigated the molecular mechanism of PD-L1 stabilization induced by CCL21.

Posttranslational modifications of PD-L1, as important regulatory mechanisms, directly influence PD-L1-mediated immunosuppression in patients with cancer.³⁹ Recently, Li et al²³ found that the phosphorylation of PD-L1 by GSK-3 β could be degraded by the ubiquitin/proteasome system, whereas CCL21 could inhibit GSK-3 β activity through the PI3K-AKT signaling pathway in colorectal cancer cells.²⁷ In addition, PI3K-AKT signaling was significantly enriched in the CCL21 highly expressed PC samples by our analysis. Thus, we postulated and confirmed that CCL21 stabilized PD-L1 protein on tumor cells through the AKT-GSK-3 β signaling pathway in this study.

The PD-L1 on tumor cells could promote T cell apoptosis *in vitro* and *in vivo* to induce immune evasion.⁹ Consequently, there was a correlation of PD-L1 expression on tumor cells with the response to ICB therapy in many preclinical studies,^{40,41} and patients with PD-L1 positive tumors had a better response rate than patients with PD-L1 negative tumors in several cancers.⁴²⁻⁴⁴ However, patients with tumors with high PD-L1 expression might be unresponsive to anti-PD-L1 treatment due to the low T cell infiltration in PC. The lack of preexisting T cell immunity seemed to induce the resistance of anti-PD-L1 therapy, which might be one of the reasons that the efficacy of PD-L1 blockade alone is limited in PC. Therefore,

facilitating T cell infiltration in PC could overcome the resistance to anti-PD-L1 treatment. In our study, PD-L1 upregulation and T cell infiltration suggested that CCL21 might sensitize PC to anti-PD-1/PD-L1 immunotherapy. Indeed, our data from the mouse model indicated that the combination of anti-PD-L1 and CCL21 therapy led to a more significant decrease in tumor sizes than monotherapies (Figure 6).

Regarding the limitation of this study, the lentiviral vector was used to overexpress CCL21 in tumor cells to mimic its intratumoral treatment, which was infeasible in clinical practice. CCL21 gene-modified DC therapy and polymer-based CCL21 delivery might be attractive strategies for further investigation in PC. Another limitation was that we only investigated the change of PD-L1 expression, and other potential immune checkpoints might also be altered in the CCL21 treatment. Further related research is needed in the future.

In conclusion, our study showed that increased CCL21 in tumor cells promoted T cell infiltration and reduced tumor burden. Chemokine CCL21 stabilized and upregulated PD-L1 expression on tumor cells through the AKT-GSK-3 β signaling pathway, which partly impaired antitumor T cell immunity, while PD-L1 blockade could rescue this immunosuppression. These findings provide a novel PC therapeutic strategy of CCL21 in combination with anti-PD-L1 treatment.

ACKNOWLEDGMENTS

This work was supported by grants from: China Postdoctoral Science Foundation (2021M690037), Shanghai Sailing Program (21YF1407100), the National Key R&D Program (2019YFC1315902), and the Clinical Science and Technology Innovation Project of the Shanghai ShenKang Hospital Development Centre (SHDC2020CR2017B).

DISCLOSURE

The authors declare that there is no conflict of interest.

ORCID

Qiangda Chen  <https://orcid.org/0000-0003-0428-5173>

Ning Pu  <https://orcid.org/0000-0002-3123-493X>

Wenchuan Wu  <https://orcid.org/0000-0001-6317-3417>

REFERENCES

- Siegel RL, Miller KD, Fuchs HE, Jemal A. Cancer statistics, 2021. *CA Cancer J Clin.* 2021;71(1):7-33.
- Kuryk L, Bertinato L, Staniszewska M, et al. From conventional therapies to immunotherapy. Melanoma treatment in review. *Cancers.* 2020;12(10):3057.
- Iams WT, Porter J, Horn L. Immunotherapeutic approaches for small-cell lung cancer. *Nat Rev Clin Oncol.* 2020;17(5):300-312.
- Morrison AH, Byrne KT, Vonderheide RH. Immunotherapy and prevention of pancreatic cancer. *Trends Cancer.* 2018;4(6):418-428.
- Suresh K, Naidoo J, Lin CT, Danoff S. Immune checkpoint immunotherapy for non-small cell lung cancer: benefits and pulmonary toxicities. *Chest.* 2018;154(6):1416-1423.
- Amaria RN, Reddy SM, Tawbi HA, et al. Neoadjuvant immune checkpoint blockade in high-risk resectable melanoma. *Nat Med.* 2018;24(11):1649-1654.
- Almquist DR, Ahn DH, Bekaii-Saab TS. The role of immune checkpoint inhibitors in colorectal adenocarcinoma. *BioDrugs.* 2020;34(3):349-362.
- Sun C, Mezzadra R, Schumacher TN. Regulation and function of the PD-L1 checkpoint. *Immunity.* 2018;48(3):434-452.
- Feng M, Xiong G, Cao Z, et al. PD-1/PD-L1 and immunotherapy for pancreatic cancer. *Cancer Lett.* 2017;407:57-65.
- Nagarsheth N, Wicha MS, Zou W. Chemokines in the cancer microenvironment and their relevance in cancer immunotherapy. *Nat Rev Immunol.* 2017;17(9):559-572.
- Gunn MD, Tangemann K, Tam C, Cyster JG, Rosen SD, Williams LT. A chemokine expressed in lymphoid high endothelial venules promotes the adhesion and chemotaxis of naive T lymphocytes. *Proc Natl Acad Sci USA.* 1998;95(1):258-263.
- Novak L, Igoucheva O, Cho S, Alexeev V. Characterization of the CCL21-mediated melanoma-specific immune responses and in situ melanoma eradication. *Mol Cancer Ther.* 2007;6(6):1755-1764.
- Liang C-M, Zhong C-P, Sun R-X, et al. Local expression of secondary lymphoid tissue chemokine delivered by adeno-associated virus within the tumor bed stimulates strong anti-liver tumor immunity. *J Virol.* 2007;81(17):9502-9511.
- Yousefieh N, Hahto SM, Stephens AL, Ciavarra RP. Regulated expression of CCL21 in the prostate tumor microenvironment inhibits tumor growth and metastasis in an orthotopic model of prostate cancer. *Cancer Microenviron.* 2009;2(1):59-67.
- Sharma S, Kadam P, Dubinett S. CCL21 programs immune activity in tumor microenvironment. *Adv Exp Med Biol.* 2020;1231:67-78.
- Lee JM, Lee MH, Garon E, et al. Phase I trial of intratumoral injection of CCL21 gene-modified dendritic cells in lung cancer elicits tumor-specific immune responses and CD8(+) T-cell infiltration. *Clin Cancer Res.* 2017;23(16):4556-4568.
- Kadam P, Sharma S. PD-1 immune checkpoint blockade promotes therapeutic cancer vaccine to eradicate lung cancer. *Vaccines.* 2020;8(2):317.
- Chen Q, Pu N, Yin H, et al. CD73 acts as a prognostic biomarker and promotes progression and immune escape in pancreatic cancer. *J Cell Mol Med.* 2020;24(15):8674-8686.
- Warde-Farley D, Donaldson SL, Comes O, et al. The GeneMANIA prediction server: biological network integration for gene prioritization and predicting gene function. *Nucleic Acids Res.* 2010;38(suppl 2):W214-W220.
- Subramanian A, Tamayo P, Mootha VK, et al. Gene set enrichment analysis: a knowledge-based approach for interpreting genome-wide expression profiles. *Proc Natl Acad Sci USA.* 2005;102(43):15545-15550.
- Newman AM, Liu CL, Green MR, et al. Robust enumeration of cell subsets from tissue expression profiles. *Nat Methods.* 2015;12(5):453-457.
- Pu N, Gao S, Yin H, et al. Cell-intrinsic PD-1 promotes proliferation in pancreatic cancer by targeting CYR61/CTGF via the hippo pathway. *Cancer Lett.* 2019;460:42-53.
- Li C-W, Lim S-O, Xia W, et al. Glycosylation and stabilization of programmed death ligand-1 suppresses T-cell activity. *Nat Commun.* 2016;7:12632.
- Huang C-Y, Wang Y, Luo G-Y, et al. Relationship between PD-L1 expression and CD8+ T-cell immune responses in hepatocellular carcinoma. *J Immunother.* 2017;40(9):323-333.
- Zhang J, Dang F, Ren J, Wei W. Biochemical aspects of PD-L1 regulation in cancer immunotherapy. *Trends Biochem Sci.* 2018;43(12):1014-1032.
- Song M, Bode AM, Dong Z, Lee MH. AKT as a therapeutic target for cancer. *Cancer Res.* 2019;79(6):1019-1031.
- Lu LL, Chen XH, Zhang G, et al. CCL21 facilitates chemoresistance and cancer stem cell-like properties of colorectal cancer cells through AKT/GSK-3 β /snail signals. *Oxid Med Cell Longev.* 2016;2016:5874127.
- Constantinidou A, Alifieris C, Trafalis DT. Targeting programmed cell death -1 (PD-1) and ligand (PD-L1): a new era in cancer active immunotherapy. *Pharmacol Ther.* 2019;194:84-106.
- Borghaei H, Paz-Ares L, Horn L, et al. Nivolumab versus docetaxel in advanced nonsquamous non-small-cell lung cancer. *N Engl J Med.* 2015;373(17):1627-1639.
- Fehrenbacher L, Spira A, Ballinger M, et al. Atezolizumab versus docetaxel for patients with previously treated non-small-cell lung cancer (POPLAR): a multicentre, open-label, phase 2 randomised controlled trial. *Lancet.* 2016;387(10030):1837-1846.
- Förster R, Davalos-Misslitz AC, Rot A. CCR7 and its ligands: balancing immunity and tolerance. *Nat Rev Immunol.* 2008;8(5):362-371.
- Hauser MA, Legler DF. Common and biased signaling pathways of the chemokine receptor CCR7 elicited by its ligands CCL19 and CCL21 in leukocytes. *J Leukoc Biol.* 2016;99(6):869-882.
- Hou YC, Chao YJ, Hsieh MH, Tung HL, Wang HC, Shan YS. Low CD8⁺ T cell infiltration and high PD-L1 expression are associated with level of CD44⁺/CD133⁺ cancer stem cells and predict an unfavorable prognosis in pancreatic cancer. *Cancers.* 2019;11(4):541.
- Ino Y, Yamazaki-Itoh R, Shimada K, et al. Immune cell infiltration as an indicator of the immune microenvironment of pancreatic cancer. *Br J Cancer.* 2013;108(4):914-923.
- Soares KC, Rucki AA, Wu AA, et al. PD-1/PD-L1 blockade together with vaccine therapy facilitates effector T-cell infiltration into pancreatic tumors. *J Immunother.* 2015;38(1):1-11.
- Lu C, Paschall AV, Shi H, et al. The MLL1-H3K4me3 axis-mediated PD-L1 expression and pancreatic cancer immune evasion. *J Natl Cancer Inst.* 2017;109(6):djw283.
- Zhang C, Li Z, Xu L, et al. CXCL9/10/11, a regulator of PD-L1 expression in gastric cancer. *BMC Cancer.* 2018;18(1):462.
- Turnquist H, Lin X, Ashour A, et al. CCL21 induces extensive intratumoral immune cell infiltration and specific anti-tumor cellular immunity. *Int J Oncol.* 2007;30(3):631-639.
- Hsu JM, Li CW, Lai YJ, Hung MC. Posttranslational modifications of PD-L1 and their applications in cancer therapy. *Cancer Res.* 2018;78(22):6349-6353.
- Wang L, Gao Y, Zhang G, et al. Enhancing KDM5A and TLR activity improves the response to immune checkpoint blockade. *Sci Transl Med.* 2020;12(560):eaax2282.

41. Xiang J, Zhang NI, Sun H, et al. Disruption of SIRT7 increases the efficacy of checkpoint inhibitor via MEF2D regulation of programmed cell death 1 ligand 1 in hepatocellular carcinoma cells. *Gastroenterology*. 2020;158(3):664-678.e24.
42. Herbst RS, Soria J-C, Kowanetz M, et al. Predictive correlates of response to the anti-PD-L1 antibody MPDL3280A in cancer patients. *Nature*. 2014;515(7528):563-567.
43. Garon EB, Rizvi NA, Hui R, et al. Pembrolizumab for the treatment of non-small-cell lung cancer. *N Engl J Med*. 2015;372(21):2018-2028.
44. Taube JM, Klein A, Brahmer JR, et al. Association of PD-1, PD-1 ligands, and other features of the tumor immune microenvironment with response to anti-PD-1 therapy. *Clin Cancer Res*. 2014;20(19):5064-5074.

SUPPORTING INFORMATION

Additional supporting information may be found online in the Supporting Information section.

How to cite this article: Chen Q, Yin H, Pu N, et al.

Chemokine C-C motif ligand 21 synergized with programmed death-ligand 1 blockade restrains tumor growth. *Cancer Sci*. 2021;112:4457-4469. <https://doi.org/10.1111/cas.15110>